Precision Timing in the CMS MTD Barrel Timing Layer with Crystal Bars and SiPMs

Francesco Santanastasio, *Sapienza Università di Roma and INFN Sezione di Roma*,

On behalf of the CMS Collaboration

***Abstract*—The Compact Muon Solenoid (CMS) detector at the CERN Large Hadron Collider (LHC) is undergoing an extensive Phase II upgrade program to prepare for the challenging conditions of the High-Luminosity LHC (HL-LHC). In particular, a new timing layer will measure minimum ionizing particles (MIPs) with a time resolution of ~30-40 ps and hermetic coverage up to a pseudo-rapidity of $|\eta| = 3$. The precision time information from this detector will reduce the effects of the high levels of pile-up expected at the HL-LHC and will bring new and unique capabilities to the CMS detector. This MIP Timing Detector (MTD) will consist of a central barrel timing layer (BTL) based on L(Y)SO:Ce crystals read out with SiPMs and two end-caps instrumented with radiation-tolerant Low Gain Avalanche Detectors (LGADs). With the goal of maximizing the detector performance within the stringent constraints of space, cost, and channel count, the BTL exploits elongated crystal bars, each read out with two SiPMs. This unusual geometry enables the instrumentation of large surfaces while minimizing the active area of the photodetectors, and thus noise and power consumption. This article presents a summary of the R&D studies carried out to optimize this crystal-based technology and key beam test results in which the target time resolution of 30 ps has been achieved.**

***Index Terms*— Large Hadron Collider, CMS, Timing Detector, Scintillation Crystals, Silicon Photomultipliers**

I. Introduction

THE standard model (SM) of particle physics is the theory that describes the fundamental particles and their interactions. To test and study the SM and search for physics beyond the SM (BSM), the Large Hadron Collider (LHC) at CERN has provided in the last years proton-proton collisions at a center of mass energy of $\sqrt{s} = 13$ TeV never reached before in hadron colliders. The data are collected by 4 experiments, including the Compact Muon Soleniod (CMS) [1].

In 2019, the LHC began a two-year shutdown to upgrade the injector complex to produce brighter proton beams. After a three-year running period at 13–14 TeV (Run-3), there will be another long shutdown of approximately 2.5 years, starting in 2024, to upgrade the optics in the interaction region to produce more tightly focused and overlapping beams at collision. The High Luminosity LHC (HL-LHC) will resume operations in 2026 reaching a luminosity of $5 - 7 \cdot 10^{34}$ cm^{-2}s^{-1}. At the end of the HL-LHC in ~ 2038 about 3000 fb^{-1} of data will be collected, a factor 10 higher than LHC, largely increasing the physics potential of the experiments.

At HL-LHC, there will be much higher collision rates that will far exceed the capabilities of the existing CMS detector, which will consequently require significant upgrades to continue to function efficiently (Phase-2 upgrade). Due to the increased instantaneous luminosity, the number of simultaneous interactions per bunch crossing (pileup) will increase from ~ 30 to $\sim 140 - 200$. For each bunch crossing recorded by CMS, there is typically only one hard interaction of physics interest, i.e. the one probing energy scales ranging from few GeV to several TeV, while the other pileup interactions represent a background noise for physics measurements. The increased pileup at HL-LHC will result in a proportional increase of the linear density of primary interaction vertices along the beam line. The CMS global event reconstruction currently relies on a track-vertex association in space, as charged particles produced in the interactions are reconstructed as tracks in the inner tracker detector. With the increased linear vertex density at HL-LHC, a large number of pileup tracks will be incorrectly associated to the primary vertex of interest, thus producing a significant degradation in most event observables.

In order to mitigate the negative impact of pileup on physics measurements, the CMS collaboration has proposed the construction of the new MIP Timing Detector (MTD) [2]. This project, recently approved, will be included in the upgrade plan for the HL-LHC era. The MTD will give timing information for charged particles (mainly minimum ionizing particles, MIPs) with 30–40 ps resolution at the beginning of HL-LHC operation in 2026, degrading slowly as a result of radiation damage to 50–60 ps by the end of HL-LHC operations. This will help to assign charged tracks to the correct interaction vertices in bunch crossings with an average of 200 collisions or more. It exploits the fact that the individual interactions within the bunch crossing do not all occur at precisely the same time but, because of the longitudinal extent of the beams, are distributed over time

Francesco Santanastasio is with Sapienza Università di Roma and INFN Sezione di Roma, Italy. (e-mail: francesco.santanastasio@roma1.infn.it).

with an spread (standard deviation) of 180–200 ps. By associating tracks from a vertex to hits and their corresponding times in the MTD, the time at which the collision vertex occurred can be reconstructed as shown in Fig. 1. Other tracks pointing roughly towards the vertex but coming at the wrong time, can be eliminated from consideration as contributing to that particular collision. The use of timing and tracking together will, therefore, give CMS excellent association of tracks to vertices even when the vertices are very close together in space. This will help to maintain the current excellent performance of the CMS detector also in the harsh

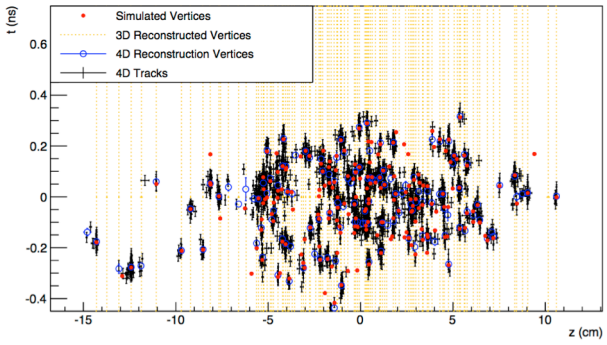

Fig. 1. Simulated and reconstructed vertices in a bunch crossing with 200 pileup interactions assuming an MTD with ~30 ps time resolution covering the barrel and endcaps of the CMS detector. The horizontal axis is the z position along the beam line while the vertical axis is the time. The simulated vertices are the red dots. The vertical yellow lines indicate 3D-reconstructed (i.e. no use of timing information) vertices, with instances of vertex merging visible throughout the display. The black crosses and the blue open circles represent tracks and vertices reconstructed using a method that includes the time information ("4D"). Many of the vertices that appear to be merged in the spatial dimension are clearly separated when time information is available. Picture from [2].

pileup conditions of HL-LHC, as shown in the example of Fig. 2.

The removal of pileup tracks inconsistent with the hard-interaction improves the reconstruction of many final state observables. For example, removing pileup tracks from the isolation cones improves the identification efficiency for isolated leptons and photons, which are key signatures of many processes of interest for the HL-LHC program (as the golden decay channel of double Higgs production, $HH \rightarrow bb\gamma\gamma$). The reconstruction of spatially extended objects and global event quantities that are vulnerable to the "pileup pollution", such as jets and missing transverse energy, will also be improved significantly. The performance of b-jet identification, which relies on vertex reconstruction, is enhanced.

In addition to preserving the quality of the data at the highest luminosities, the MTD also brings new capabilities to CMS. The identification of charged hadrons as pions, kaons, or protons based on time-of-flight becomes possible up to a few GeV in transverse momentum, which is of significant benefit to Heavy Ion physics and for specialized QCD studies in pp collisions. In addition, the ability to reconstruct the time of displaced vertices will provide enhanced capability in searching for new long-lived particles (LLPs) by measuring their relativistic velocity parameter, and, in certain cases,

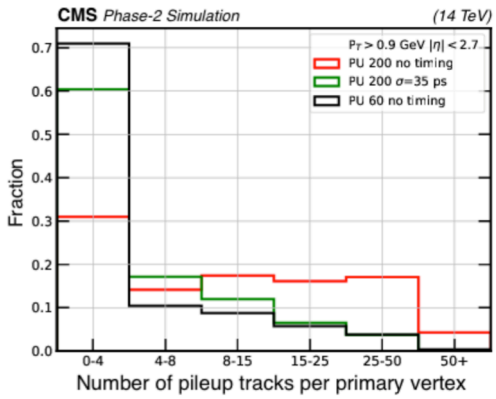

Fig. 2. Distribution of the number of incorrectly associated tracks with the use of a 3 σ (where $\sigma = 35$ ps) selection on timing information and without use of timing information ("no timing" label). The vertical axis is the fraction of primary vertices which have the number of pileup tracks shown on the horizontal axis associated to them. The label "PU 200 (60)" refers to a scenario with an average of 200 (60) pileup interactions. The black line corresponds to conditions similar to the current LHC. Picture from [2].

permitting the reconstruction of the LLP's mass.

The MTD will be divided into two sections with an almost hermetic coverage: the Barrel Timing Layer (BTL) will cover the central part of the timing detector while the Endcap Timing Layer (ETL) will cover the forward region, as shown in Fig. 3. At the end of HL-LHC (about 3000 fb^{-1} of data collected) the detectors will have received radiation doses of 20-30 kGy in the barrel and between 20 and 450 kGy in the endcaps. The two detector layers will use different sensor technologies: scintillator crystals readout by silicon photomultipliers in the barrel, and low gain avalanche detectors (LGADs) in the endcaps. This division is driven by several considerations, including significant difference in integrated radiation dose at the HL-LHC between the two sections, accessibility for maintenance, time schedule, and costs. This article will focus on the description of the BTL,

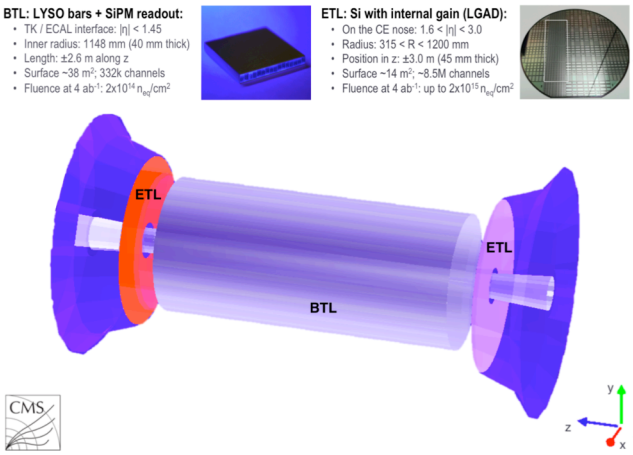

Fig. 3. A schematic view of the MTD detector comprising a barrel layer (BTL, grey cylinder), at the interface between the tracker (inside the BTL volume and indicated as "TK") and the electromagnetic calorimeter (outside the BTL volume and indicated as "ECAL"), and two silicon endcap timing layers (ETL, orange and light violet discs) in front of the endcap calorimeter (indicated as "CE"). Picture from [2]. More details on the detector design are also reported in Ref. [2].

providing the status of the R&D and the plans for the operation of this detector at the HL-LHC.

II. The Barrel Timing Layer

A. Geometry of the detector

The Barrel Timing Layer is a thin, cylindrical detector that will be housed inside the tracker support tube of the CMS experiment. The inner boundary of its radial envelope is 1148 mm from the beam and the outer boundary is at 1188 mm, for a maximum radial extent of 40 mm. Its overall active length in z is about 5000 mm. To satisfy the requirements related to tight construction schedule and limited accessibility during the HL-LHC period, it was decided to choose technologies for the sensor that have well-established production and assembly procedures and facilities in industry, and with which CMS has past experience.

The fundamental detecting cell will consist of a thin LYSO:Ce scintillator crystal bar of about 5.7 cm in length oriented along the φ direction in CMS, a width of 3.0 mm along the z direction, and a variable radial thickness (from 3.7 mm in the central region to 2.4 mm in the forward region) in order to maintain an approximately constant slant depth crossed by particles coming from the interaction point. Each end of the 165888 crystal bars will be coupled to a silicon photomultiplier (SiPM) whose dimensions will be 3 mm along φ and a variable thickness, chosen to approximately match the bar's radial thickness in each region. The choice of a bar geometry is strategic for the detector optimization since the light collection efficiency (LCE) in this case relies mostly on optical photons that are collected within the angle of total internal reflection. The readout of both ends of the bar provides two measurements of the time of arrival of a MIP that are combined to eliminate the effect of the time delay of the light traveling along the crystal and to improve the time resolution.

The detector is divided longitudinally into $+z$ and $-z$ end (where z represents the spatial coordinate along the beam line) of length 2.6 m, each end consisting of 36 azimuthal segments, which span 10° each. Each azimuthal segment has a row of six Readout Units (RUs), supporting 4608 SiPMs in a unit called a tray. In all, the 72 trays contain 331776 SiPMs (total number of readout channels). Figure 4 shows the different components of the BTL.

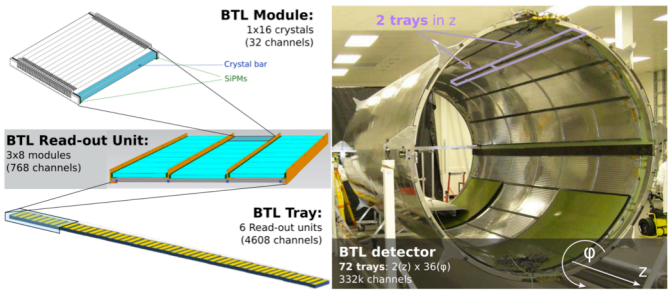

Fig. 4. Overview of the BTL showing (left) the hierarchical arrangement of the various components, bars, modules, and Readout Units, and (right) trays (purple rectangles near the top), inside the tracker support tube. Picture from [2].

B. LYSO crystals

For precision timing purposes in the BTL environment, LYSO:Ce crystals (i.e. $(Lu_{1-x}Y_x)_2SiO_5$ with fraction x below 20%) represent an optimal candidate compared to other inorganic scintillators because of their high light yield (LY) of about 40000 photons/MeV, fast scintillation rise time (τ_r<100 ps), and relatively short decay time ($\tau_d \sim 40$ ns). Basic principles of scintillation mechanism in inorganic crystals are discussed in Ref. [3]. The figure of merit for precision timing is the number of photons produced within a short time window of about 500 ps from the beginning of the scintillation signal (early photons), which for LYSO:Ce is about 400 photons/MeV. Given the high density of LYSO (~7.1 g/cm^3), about $E_{dep} \sim 4$ MeV are deposited in the crystal by a MIP traversing the BTL giving more than 1500 "early photons". Finally a key feature of LYSO:Ce is its radiation tolerance [4], [5], [6] which is required for operation without significant loss of transparency or light output in the high radiation environment until the end of HL-LHC operation.

The LYSO:Ce crystals are mass produced by a large variety of vendors worldwide. The qualification of the crystals will be performed during 2019-2020 and will include a thorough validation of single crystal bars and crystal modules from about 10 vendors. The crystal characterization will consist in several measurements including light output, time resolution, decay time, optical isolation of crystals within a module, and dimensions. Figure 5 shows some LYSO crystal bars of different thickness and a crystal module together with silicon photomultipliers.

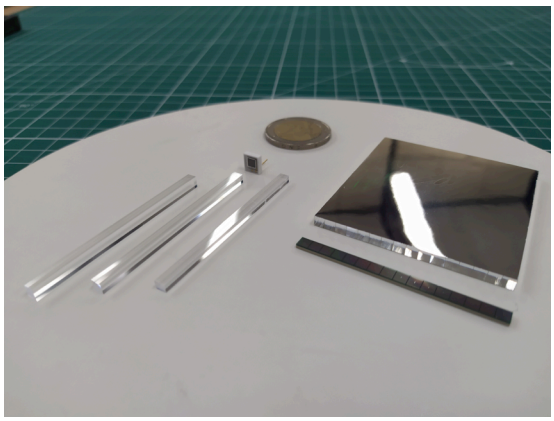

Fig. 5. LYSO crystal bars of different thickness (left) and a crystal module made of 16 bars (right). A single SiPM (left) and a SiPM array (right) are also shown. The BTL will be made of crystal modules coupled to SiPM arrays. A coin is also shown at the top for size comparison.

C. Silicon Photomultipliers (SiPMs)

The photo-sensors of choice for the BTL are silicon photomultipliers (SiPMs). SiPMs are compact, robust, and insensitive to magnetic fields. They can be exposed to room light without damage and operate at relatively low voltages, on the order of 30–77 V, with low power consumption. A photo-detection efficiency, PDE, of up to 40% is achievable in devices with small cell size (15 μm square pixels). Small cell sizes also extend the linear range of the SiPM and, combined

with a fast cell recovery time, enhance its performance after irradiation. Finally, large quantities of SiPMs can be fabricated in industry with excellent uniformity and acceptable cost. Different SiPM technologies are under consideration for BTL, including the NUV-HD (thin-epi) SiPM from Fondazione Bruno Kessler (FBK) and the S12572 and HDR2 from Hamamatsu Photonics (HPK) with cell pitch of 15 μm.

SiPMs operate above the breakdown voltage in Geiger mode with a gain of the order of 10^5-10^6. The over-voltage (OV), the difference between the operating bias voltage and the breakdown voltage, produces a dark current that grows as the radiation dose accumulates. In order to mitigate the negative effects of dark count rate (DCR) different approaches can be followed:

- *Cooling*. Since dark current increases by roughly a factor of two for each increment of $7-10$ ℃, the SiPMs will be operated at low temperatures of about -30 ℃. This results in the need for substantial cooling power.
- *Bias voltage reduction*. Because the OV also controls the photon detection efficiency (PDE), there is a tradeoff between noise rate and signal amplitude, and therefore time resolution. The SiPM operation voltage will have to be smoothly decreased by about 3 V during the detector lifetime to limit the noise level while maintaining good time resolution. The decrease of the overvoltage will imply a reduction of the PDE and therefore a degradation of the time resolution during the detector operation.
- *Annealing*. The radiation damage induced in silicon consists of different types of defects, each having a characteristic recovery time. Spontaneous annealing of the radiation induced current has been observed on irradiated SiPMs [7] and from the first tests it appears to follow a behavior similar to that of APDs described in Ref. [8]. Periods of SiPM annealing at room temperature are foreseen during shutdowns. Different scenarios are shown in Fig. 6.

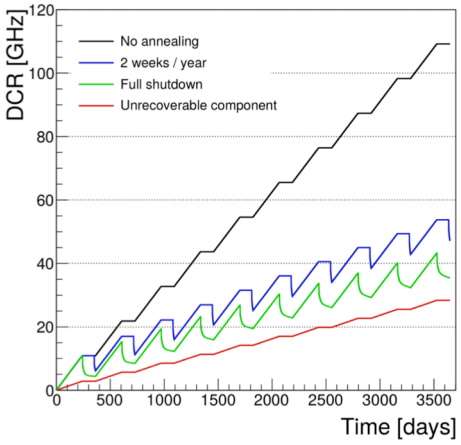

Fig. 6. Expected growth of dark count rate (DCR) for an Hamamatsu SiPM S12572 for various annealing scenarios at room temperature and at fixed OV of 1.5 V during the detector lifetime. The model used in this projection is based on the measurements reported in Ref. [7-8]. Picture from [2].

III. Test Beam Results

BTL sensor prototypes have been tested and characterized at the test beam facilities of CERN and Fermilab with the goal of proving that the design time resolution of 30ps could be reached.

At CERN, 80 GeV pions were used as a well calibrated source of minimum ionizing particles. In a typical setup, the pion beam first passes through hodoscope planes which provides particle tracking with a spatial resolution of the order of the millimeter, then through a Micro Channel Plate (MCP) with time resolution of about 16 ps used as timing reference, and finally it crosses a single LYSO crystal bar under test (with the long bar side placed orthogonally to the beam direction) readout by one SiPM at each end. The two SiPMs are indicated with the "Left" and "Right" labels in the following.

Figure 7 shows the time difference between the signal of a SiPM (Left or Right) and the reference time of the MCP signal as function of the impact point of the pion along the bar. The arrival time of the signal on a SiPM is proportional to the distance between the SiPM and the point where the scintillation photons are emitted along the X direction, showing that the device is sensitive to the light propagation in the bar. The plot also shows the average time $t_{ave} = \frac{t_L+t_R}{2}$ which is independent on the impact point and represents the best estimate of the signal time measured by the bar as a whole, as discussed later. The slope of Fig. 7 for Left and Right SiPMs shows that the propagation speed of signal along the bar is about 0.1 mm/ps, comparable with the speed of light in LYSO and thus indicating that the scintillation photons follow an almost direct path to SiPMs within the total internal reflection cone. From the time difference between the Left and Right SiPM it is therefore possible to reconstruct the impact point of the charged particle with a resolution of about 3 mm (assuming a time resolution of 30 ps on t_{ave}), thus showing the tracking capabilities of the BTL detector.

Figure 8 shows the time resolution of the LYSO detector (after subtracting the contribution from the reference MCP) as function of the impact point of the charged particle along the bar in three different cases: Left and Right SiPM only, and using the average time of the two, t_{ave}. The combination of time information from the two statistically uncorrelated SiPMs, provides a uniform time response and an improved time resolution by a factor $\sqrt{2}$ compared to the individual SiPM measurements. The results of this study show that the BTL design time resolution of 30 ps can be reached using LYSO bars readout by SiPMs.

IV. Time Resolution

A minimum ionizing particle traversing the crystal volume will produce a number of optical photons along its track proportional to the crystal light yield (LY) defined as the number of photons generated per MeV of energy deposit. A fraction of the photons will be detected at each SiPM. Detected photons will be converted to photoelectrons and

amplified by the SiPM, operated with a gain of O(10^5-10^6), to generate an electrical signal that can be discriminated and digitized to obtain a measurement of the time at which the MIP crossed the detector, referred to as the "time stamp".

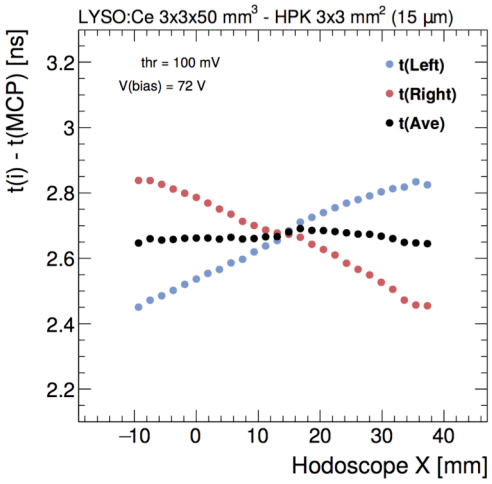

Fig. 7. Time stamp from the Left and Right SiPMs and average time stamp t_{ave}, tave, as a function of the impact point X along the crystal bar axis. Picture from [2].

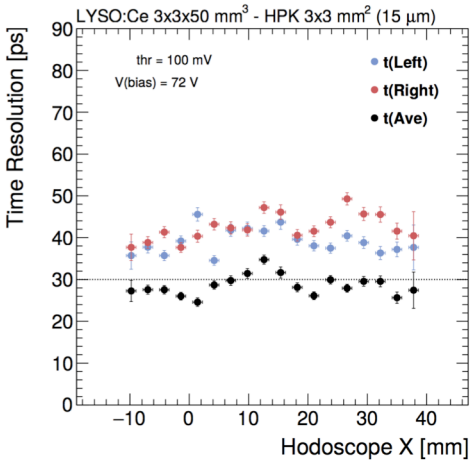

Fig. 8. Time resolution for the Left and Right SiPMs and average time stamp t_{ave} as a function of the impact point X along the crystal bar axis. Picture from [2].

Along this detection chain several effects can introduce stochastic and systematic fluctuations that lead to a degradation of the detector time resolution. The time resolution per track, from the combination of two independent measurements at the two ends of the crystal with a common clock jitter, is given by the sum in quadrature of the following terms:

- CMS clock distribution: 15 ps;
- Digitization: 7 ps;
- Electronics: 8 ps;
- Photo-statistics: 25-30 ps;
- Noise (SiPM dark counts): negligible at start-up, 50 ps after 3000 fb^{-1}.

The timing performance drivers are the photo-statistics and the noise term, thus major R&D efforts have been spent on their optimization.

The contribution from photo-statistics is related to the stochastic fluctuations in the time-of-arrival of photons detected at the SiPM, and its scaling with respect to key BTL parameters introduced above in the text is summarized by the equation [9]:

$$\sigma_t^{phot} \propto \sqrt{\frac{\tau_r \tau_d}{N_{photoele}}} \propto \sqrt{\frac{\tau_r \tau_d}{E_{dep} \cdot LY \cdot LCE \cdot PDE}} \quad (1)$$

where τ_r , τ_d , E_{dep} , LY, LCE and PDE are, respectively, the rise and decay time of the scintillation signal, the energy deposited in the crystal, the light yield of the scintillator, the light collection efficiency and the photon detection efficiency of the SiPMs.

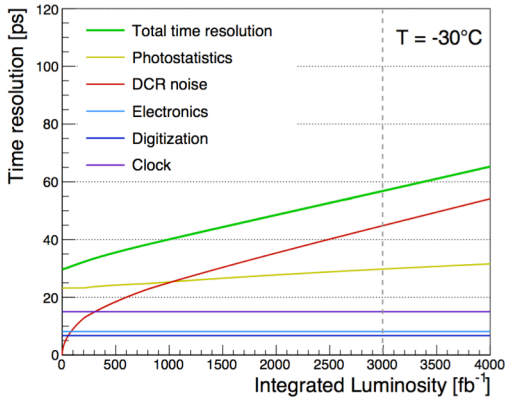

Fig. 10. Evolution of different terms contributing to the BTL time resolution as a function of integrated luminosity. The two time measurements from the SiPMs at the opposite ends of a LYSO:Ce crystal bar are combined in a single measurement. The curves are calculated for the SiPM type HDR2-015 from Hamamatsu and include the expected bias voltage reduction in time as well as a standard annealing scenario. Picture from [2].

The contribution due to the noise term scales with the dark count rate (DCR) in the SiPM proportionally to $\sqrt{DCR}/N_{photoele}$. The magnitude of the DCR increases with integrated luminosity due to radiation damage creating defects in the silicon, as discussed above.

The relative contribution of all these terms to the total time resolution is shown in Fig. 10 as function of the time from the start of BTL detector operation. While at the beginning the time resolution will be driven by the stochastic term, at about 1/3 of the HL-LHC run the DCR noise term will become dominant. A time resolution between 30 and 60 ps will be maintained during the whole lifetime of the BTL detector, which is enough to have a significant impact on the event reconstruction and therefore on the physics measurements.

V. Physics Impact Example: Di-Higgs Production

There are three main different ways of exploiting the MTD to improve physics impact: by using physics objects with improved performance from the time information; by improving the discrimination power through the use of new, time-based variables; and by using the new particle identification capabilities provided by time-of-flight measurements exploiting the MTD. Three families of analyses have been considered to cover these aspects: the search for Higgs boson pair (HH) production in several final states; the search for long-lived particles (LLP) in "beyond the standard model" (BSM) models; the measurement of heavy flavor hadron production in Heavy Ion collisions. More details on these studies are reported in Ref. [2].

In this section, special focus is given to the precision characterization of the Higgs boson, which will be one of the highest priorities of the HL-LHC physics program. In particular the study of the HH production constitutes the only way to directly determine the value of the Higgs boson trilinear self-coupling and thus determine the shape of the Brout–Englert–Higgs potential and explore the nature of the scalar sector of the SM. Five decay channels have been explored and combined: bbbb, bb$\tau\tau$, bbWW (WW $\rightarrow$ lνlν with l = e or μ), bb$\gamma\gamma$, and bbZZ (ZZ $\rightarrow$ 4l with l = e or μ). The richness and variety of physics objects spanned by this analysis makes it sensitive to the individual improvements in each of them.

The inclusion of MTD information in the physics objects has a large, integral effect in its final experimental reach. Assuming 3000 fb^{-1} of data and an average resolution of 35 ps, the MTD will bring an expected improvement to the significance of HH signal of about 13%, which would require an additional 26% luminosity without MTD. Even in a conservative scenario with a time resolution of 50 ps the MTD is expected to provide a performance gain that would require an equivalent additional luminosity of about 20% for the CMS detector without MTD to be achieved. This preliminary study only includes the cumulative benefits from improved charged lepton isolation sums and b-tagging. Additional gains in sensitivity will also come from the improved pileup rejection in final states with jets or from the improved missing transverse energy resolution in the bbWW and bb$\tau\tau$ channels.

VI. Conclusion

The CMS upgrade for HL-LHC will include a new Mip Timing Detector (MTD) to measure the time of flight of charged particles with a design time resolution of 30 ps and an hermetic coverage. The full CMS physics program will benefit from this new detector. The MTD will mitigate the negative impact on physics measurements of the harsh pileup conditions at HL-LHC. As a result of the improved event reconstruction, many interesting physics channels (such as the yet unobserved production of two Higgs Bosons) will benefit from an effective increase in integrated luminosity by about 20-30% compared to a CMS experiment without the MTD. Finally this new timing detector will provide novel identification capabilities for low energy charged particles and will open new possibilities in the search for long-lived particles predicted by several theories beyond the standard model. The Barrel Timing Layer (BTL) will be made by LYSO:Ce crystal bars readout by SiPMs. These represent well established technologies thanks to past R&D. The design target resolution of 30 ps was proved in test beams. The LYSO crystal and SiPM qualification is ongoing and the BTL detector construction will start around 2021 accordingly with the current schedule.

Acknowledgment

The author would like to thank the all SCINT2019 organizers for very interesting physics program and the beautiful conference location of Sendai in Japan.

References

[1] The CMS Collaboration, "The CMS Experiment at the CERN LHC", *JINST.*, vol. 3, pp. S08004, Aug. 2008.

[2] The CMS Collaboration, "A MIP Timing Detector for the CMS Phase-2 Upgrade", CERN-LHCC-2019-003 or CMS-TDR-020, Mar. 2019. Available: https://cds.cern.ch/record/2667167.

[3] Piotr A. Rodnyi, "Physical processes in inorganic scintillators", Boca Raton; New York : CRC press, May 1997.

[4] E. Auffray *et al.*, "Radiation damage of LSO crystals under γ and 24 GeV protons irradiation", *Nucl. Instrum. Meth. A,* vol. 721, pp. 76-82, Sep. 2013.

[5] F. Yang, L. Zhang, and R. Y. Zhu, "Gamma-ray induced radiation damage up to 340 Mrad in various scintillation crystals", *IEEE Trans. Nucl. Sci.,* vol. 63, pp. 612–619, Apr. 2016.

[6] F. Yang *et al.*, "Proton induced radiation damage in fast crystal scintillators", *Nucl. Instrum. Meth. A*, vol. 824, pp. 726-728, Jul. 2016.

[7] E. Garutti and Y. Musienko, "Radiation damage of SiPMs", *Nucl. Instrum. Meth. A* vol. 926, pp. 69-84, May 2019.

[8] The CMS Collaboration, "The CMS electromagnetic calorimeter project: Technical Design Report", *Technical Report CERN-LHCC-97-033.* CMS-TDR-4, CERN, Geneva, 1997.

[9] S. Vinogradov, "Approximations of coincidence time resolution models of scintillator detectors with leading edge discriminator", *Nucl. Instrum. Meth. A*, vol. 912, pp. 149-153, Dec. 2018.